20th International Conference on Advances in ICT for Emerging Regions (ICTer 2020): 190 - 195

Single Image Defogging using Depth Estimation and Scene-Specific Dark Channel Prior

T. Kokul
Department of Physical Science
Vavuniya Campus of the University of Jaffna
Sri Lanka
kokul@vau.jfn.ac.lk

S. Anparasy
Department of Physical Science
Vavuniya Campus of the University of Jaffna
Sri Lanka
anpusuji@gmail.com

2020 20th International Conference on Advances in ICT for Emerging Regions (ICTer) | 978-1-7281-8655-9/20/$31.00 ©2020 IEEE | DOI: 10.1109/ICTer51097.2020.9325450

***Abstract*— Quality of outdoor images are often degraded under bad weather conditions by the extensive presence of suspended particles in the atmosphere such as fog and haze. Although, many single image defogging approaches have been proposed in the past, their restoration performance is considerably low since they fail to consider the image-specific cues. To feed that information, we propose a simple and robust defogging framework that can estimate the rough depth map of a foggy image based on the density of the fog in local regions. Obtained depth map information is used to compute the scene-specific dark channel and transmission. In addition, a histogram normalization based post-processing technique is used to enhance the restoration. Experimental evaluation performed on a benchmark dataset demonstrates the proposed defogging framework outperforms state-of-the-art approaches.**

Keywords—Defogging, Dark Channel Prior, Image Enhancement

I. INTRODUCTION

Poor visibility in outdoor images is one of the key challenge in many image understanding and computer vision-based applications such as traffic monitoring[3], automated driving[4], object detection[5], object tracking[6], and aerial imagery[7]. Bad weather conditions, such as fog, haze, cloud and mist, can significantly reduce the visual quality of outdoor images. One of the major reasons for vehicle accidents is poor visibility due to the foggy scenes. The objective of the defogging frameworks is to increase the visual quality of foggy scenes by restoring the details and colour.

Fog is caused by the extensive presence of water droplets in the air due to the bad weather conditions. These water droplets scatter the sunlight and light reflected from other objects. Due to the scattering, contrast of an outdoor scene will be faded, and a whiteness effect will be produced towards the observer or camera. These two effects jointly produce a poor-quality image. It is observed that[8, 9] the amount of fog in an image mainly depends on the distance between the scene and camera. Therefore, estimating the depth map of a foggy image is important for restoring the fog-free image.

Single image fog removal is a challenging task since fog is dependent on the unknown depth. Depth map prediction is a challenging problem if the input is only a single image. Therefore, many defogging approaches have used multiple images and additional information[10, 11] to recover the details. However, without any prior information, single image fog removal in real-time is the demand of many real-world applications such as automated driving systems and vision-based surveillance systems.

Single image fog removal has attracted much research in the past [1, 9, 11-19] and following two major strategies. First group of approaches[16-18, 20] use a trainable machine learning technique to model the depth map of foggy scenes. These models recover the foggy image patches by learning the knowledge from similar foggy image samples. Although, such methods show significant recovering accuracy, their computational cost is much expensive and therefore not suitable for many real-time applications.

The second group of frameworks use the simple but efficient image enhancement methods, without any machine learning techniques. Most of the early works used several traditional image enhancement techniques such as median filtering[21], white balance correction[15], histogram equalization[22], and edge smoothing[23]. These methods are simple, fast, and can be used for real-time applications. However, since they apply the enhancement techniques without considering the actual factors which causes poor quality in foggy images, their performances are limited and even may distort the actual colour information.

Recently, few image enhancement based approaches[2, 14] showed significant improvement in single image defogging by using stronger priors or assumptions. Based on the observations of a large number of foggy and fog-free images, the 'dark channel prior'[14] framework has been proposed and showed state-of-the-art performance. This approach lies on the observation of intensities of few pixels are close to zero in at least one colour channel in a local patch of a fog-free image. Conversely, this observation does not exist in foggy images, and hence the scene can be recovered by estimating the thickness of the fog. Although, the 'dark channel prior' approach is simple and effective, it applies the same defogging algorithm on all over the image without considering the depth map, which leads to distortion in recovered images, especially in dense foggy regions.

A robust single image fog removal framework should have state-of-the-art recovering performance in real-time and computationally efficient, since which are the requirements of many real-world applications. To achieve this objective, we propose a novel defogging framework based on image enhancement techniques. It relies on the assumption of rough depth map of a foggy image can be obtained by measuring the thinness of fog in local patches of an image. In the initial stage, the proposed approach measures the thickness of fog and then the rough depth map is obtained by using a superpixel-based segmentation technique. The captured depth map information is then used to feed the scene-specific information in dark channel prior algorithm. Proposed approach showed state-of-the-art performance on a publicly available benchmark dataset.

II. Related Work

For several years, a large number of single image defogging and dehazing frameworks have been proposed and their performance have been evaluated on various benchmarks[24, 25]. The most relevant single image defogging frameworks and techniques are discussed in this section. Comprehensive reviews on these frameworks can be found in [9, 26-28].

The initial defogging frameworks are focused on image enhancement without any knowledge of the fog model. Apurva et al., [21] used gamma transmission and median filtering for defogging. Xu et al., [22] used an adaptive histogram equalization technique to recover the colour foggy images. Also, several other enhancement methods used in the past such as wavelet transform, edge smoothing, and Retinex theory. These approaches tried to enhance the brightness and contrast features in foggy images. However, their performances are limited since they fail to consider why the visual quality of foggy image is degraded.

Recent defogging and dehazing approaches rely on certain prior knowledge or observations. Kaiming He et al., [14] proposed a novel single image dehazing approach, referred to as Dark Channel Prior (DCP). They found that, in most local patches of a fog-free image, intensities of few pixels in at least one colour channel are very low. With this observation, they estimate the thickness of fog, and proposed a restoring algorithm. DCP is simple and efficient in most cases.

DCP approach has drawn a grate attention in the image enhancement community and many follow-up approaches have been proposed[1, 2, 8, 12, 13, 15, 29, 30]. Few approaches[13, 30] improve the recovering performance and speed of DCP by introducing a new smoothing filter, called as guided filter. Renjie He et al.,[15] proposed a white balance correction technique to refine the DCP algorithm. Shunyuan Yu et al.,[12] included a multiple transmission layer fusion technique to enrich the performance of DCP. Chunlin Chen et al.,[29] replaced the global parameters of DCP by a location based local parameter settings. Qingsong et al., [2] proposed a colour attention prior model based on the inspirations of DCP. Jin-Hwan et al.,[1] proposed a contrast enhancement technique for defogging in images and video. Anwar and Arun[8] proposed a novel post-processing technique in DCP.

Although DCP based single image defogging approaches are simple and computationally efficient, there is still a considerable recovering performance gap observed when these approaches are evaluated on benchmark datasets. Our objective is to reduce this performance gap by including the depth map information in DCP algorithm without using any machine learning model as they are computationally expensive.

III. Background

A. Atmospheric Scattering Model

In computer vision and graphics, the formation of fog or haze in an image is described by an atmospheric scattering model[31]. In this model, fog is treated as a combination of two components: Direct attenuation and Airlight. Attenuation diminishes the contrast and Airlight adds a whiteness effect in a foggy image. Based on that, the formation of fog is expressed as:

$$\mathbf{I}(x) = I_{Attenuation}(x) + I_{Airlight}(x) \quad (1)$$

Where x is the location of a pixel within the image, **I** is the observed foggy image, and $I_{Attenuation}$ and $I_{Airlight}$ are the attenuation and airlight on that location, respectively. The attenuation describes the scene radiance (i.e. the fog-free image that we want to recover) and medium transmission. Airlight is the scattered light that leads to the shift of the scene colours. The both components can be expressed by the following equations:

$$I_{Attenuation}(x) = \mathbf{J}(x)\, t(x), \quad (2)$$

$$I_{Airlight}(x) = \mathbf{A}\,(1 - t(x)), \quad (3)$$

Where **J** is the scene radiance, **A** is the atmospheric light, and t is the transmission parameter, which indicates the part of the light that penetrates through the fog. The transmission parameter t depends on the distance between the scene and camera, and it can be described as:

$$t(x) = e^{-\beta d(x)}, \quad (4)$$

Where β is the scattering coefficient and d is the depth of the scene. The objective of any defogging framework is to obtain **J, A** and t from **I.** To obtain these values, several assumptions and prior knowledge are utilised in many single image defogging frameworks.

B. Dark Channel Prior

In this section, the Dark Channel Prior (DCP)[14] algorithm is reviewed, since we make use of it as the baseline defogging framework. DCP is simple and computationally efficient, and therefore many of the recent defogging and dehazing frameworks make use of it as their baseline.

DCP works only for colour images and is built based on the concept of a dark channel. In an image, its dark channel J^{dark} can be defined as:

$$J^{dark}(x) = \min_{y \in \Omega(x)} \left(\min_{c \in \{r, g, b\}} J^c(y) \right), \quad (5)$$

Where $\Omega(x)$ is a local image patch centred at x and J^c is the colour channel of J. The authors of DCP assume that the transmission is constant in the local patch $\Omega(x)$. Based on their observation on a large number of fog-free images, the intensity of dark channel is tends to be zero, except the sky regions as:

$$J^{dark} \rightarrow 0, \quad (6)$$

This observation is called as *dark channel prior*. Based on that, the transmission can be derived as:

$$t(x) = 1 - \omega \min_{y \in \Omega(x)} \left(\min_{c} \frac{I^c(y)}{A^c} \right), \quad (7)$$

Where ω ($0 \leq \omega \leq 1$) is the defogging parameter that will control the degree of fog removal. The DCP algorithm assumes that the brightest pixel in **I** is approximately equals to **A**. Based on these assumptions and equations, the scene radiance **J** can be described as:

$$\mathbf{J}(x) = \frac{\mathbf{I}(x) - A}{\max(t(x), 0.1)} + A, \quad (8)$$

The performance of DCP defogging framework is mainly depends on its key parameters: Patch size (Ω) and defogging parameter ω. The dark channel concept becomes stronger for larger values of Ω because possibility of a large patch contains

(a) (b)

Fig.1. DCP approach [12] shows poor performance (unnatural effect) in brighter regions. (a) Foggy image. (b) Recovered image.

a dark pixel is increased. On the other side, DCP built on the assumption of transmission is consent in a patch, and hence large Ω produces halos in near depth scenes. Therefore, based on the experiments, patch size Ω is fixed to 15 ×15 in DCP and other follow-up approaches. We have observed that Ω should be as much as large in constant transmission regions to get the better dark channel. Based on the equation (4), amount of transmission is same in equal depth regions. Therefore, patch size Ω should be fixed locally, based on the depth map of a foggy image.

The other key parameter ω is used to control the degree of fog removal in the DCP approach. The value of ω is fixed to 0.95 in DCP and other approaches, since if the entire fog is removed from a foggy image, the recovered image may seem unnatural. However, based on our observations, ω should be large in dense foggy regions and be small thin foggy regions. Otherwise, as shown in Fig.1, it causes unnatural effect in the recovered image. Since the density of the fog depends on the depth map, value of ω should be fixed locally, based on the depth map of a foggy image.

We have also notice that DCP and follow-up approaches show poor performance in brighter regions because they apply fixed values for the both key parameters. To overcome the limitations of DCP and other dark channel prior based approaches, we propose a novel single image defogging framework by capturing and including the scene-specific information.

IV. METHODOLOGY

The key objective of the proposed framework is to include the scene-specific knowledge to the dark channel prior based defogging to increase the restoring performance. In the initial stage, the proposed approach estimates the rough depth map of the foggy image based on the density of the fog in local regions. Then the obtained rough depth map is used to calculate the scene-specific patch sizes (Ω) and defogging parameters (ω) for corresponding individual local regions. Based on the local values of these parameters, scene-specific dark channel is obtained and then the scene-specific adaptive transmission is estimated. In the post-processing, we use a colour balancing mechanism to enhance the quality of recovered image. The overview of the proposed framework is shown in Fig.2. The details of each steps are explained in the following subsections.

A. Depth Map Estimation

Estimating the depth or geometry of a scene from a single image is one of the major problems in several computer vision based applications. Without a machine learning technique, propose a depth estimation model is a challenging task, since the appearance information is insufficient to resolve depth ambiguities. However, machine learning based depth estimation techniques are computationally expensive and hence not suitable for real-time single image fog removal. In this background, we focused to develop a simple but efficient depth map estimation technique based on some prior assumptions and observations in foggy images. The proposed technique identifies the distinct depth regions in a foggy image and then that knowledge is used to improve recovering performance of the proposed defogging framework.

We have observed that density of fog is peak in depth scenes and low in close objects. We have also notice (Fig.3 (a)) that the intensity of dark channel gives the rough approximation of the thickness of the fog. Based on these observations, we assume that rough depth map of a foggy image can be estimated by the intensity of the dark channel.

In the proposed depth map estimation technique, a 3 × 3 patch is used to obtain the dark channel of the foggy image and hence the intensity of obtained dark channel is considered as the density of the fog in that image. We have used an image segmentation technique to identify and group equal depth pixels in the obtained dark channel.

Superpixel based image segmentation algorithms group the adjacent pixels based on their intensity values and then identify the distinct regions. Since superpixel based segmentation algorithms are simple, fast, and efficient, we have utilised it to identify the distinct depth regions. We have followed the 2D superpixel based segmentation algorithm of Achanta et al.,[32] to obtain the distinct depth map regions. Fig.3. visualizes the proposed depth map estimation technique in a foggy image.

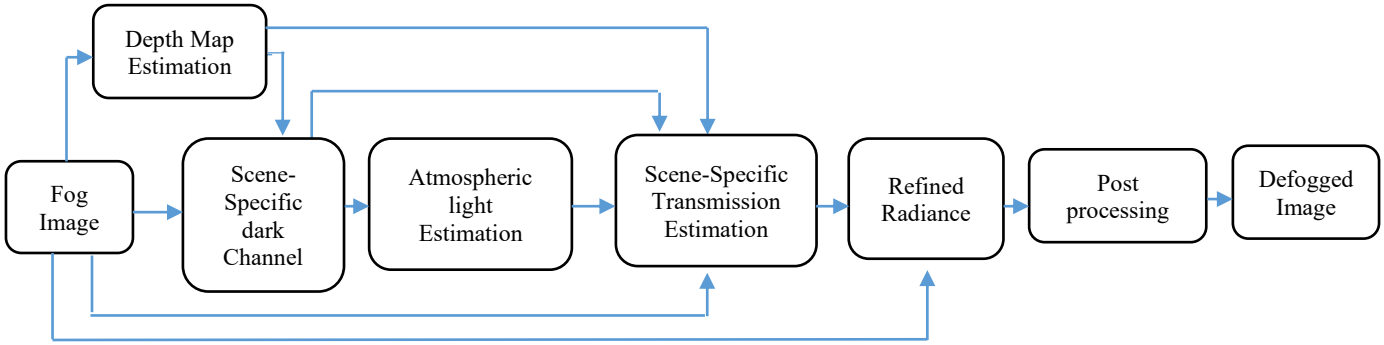

Fig.2. Flow diagram of the proposed framework. It feeds the scene-specific information into the dark channel prior based algorithm by estimating the rough depth map at the initial stage, and then used it to find the scene-specific dark channel and estimate the adaptive transmission.

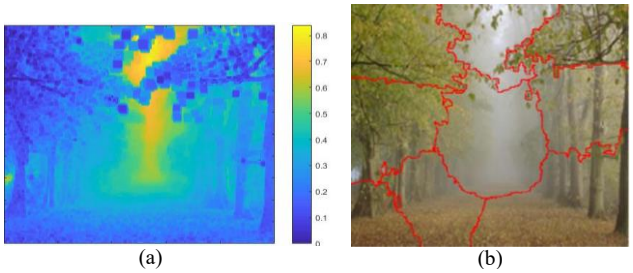

(a) (b)

Fig.3. Depth estimation in foggy image. (a) density of fog based on the dark channel. (b) Identified equal depth regions by using the superpixel based segmentation. Boundaries of the regions are shown in red colour.

At the initial stage of the proposed approach, depth distinct regions are identified and then that information is used to feed the scene-specific knowledge in defogging.

B. Scene-Specific Dark Channel

Defogging performance of DCP and all follow-up approaches are mainly depending on the dark channel estimation. In all these approaches, dark channel of a foggy image is computed (based on equation 5) by assuming the transmission is constant within a local patch. All approaches are used a 15×15 patch (**Ω**) without considering any depth information of the image.

It is observed that dense fog regions are brighter than thin fog regions due to the additive airlight. We have also notice that probability of a dark pixel is lower in brighter regions. Based on these observation and fact, we have proposed a novel technique to get the robust dark channel, which is called as scene-specific dark channel. This proposed technique lies on the assumption of large patch sizes are desirable in dense fog regions since these regions are much brighter and hence the probability of a dark pixel is much lower.

TABLE 1. Average intensities of regions and corresponding patch size.

Average Intensity (I_i)	**Patch Size (Ω)**
$I_i \geq 240$	21 × 21
$240 > I_i \geq 140$	15 × 15
$140 > I_i \geq 90$	11 × 11
$I_i < 90$	5 × 5

From the initial step of the proposed framework, depth regions were identified. We have used that regions to feed scene-specific knowledge in dark channel computation. Firstly, average intensity (I_i) values of each regions are calculated, and then these values are considered as the density of fog in that regions. Based on the average intensity values, we have fixed the patch size for each region. Large patch size is fixed for high density regions while small size is fixed for low density regions. The details of this assignment are described in Table 1.

In a local region r, its dark channel J_r^{dark} is calculated as:

$$J_r^{dark}(x) = \min_{y \in \Omega(x)} \left(\min_{c \in \{r, g, b\}} J^c(y) \right), \qquad (9)$$

Where Ω (x) is a local image patch centred at x in region r, and J^c is the colour channel of J. Then, the overall dark channel of an image is calculated as:

$$J^{dark} = J_1^{dark} \cup J_2^{dark} \ldots \cup J_n^{dark} \qquad (10)$$

Fig.4. Effectiveness of the proposed scene-specific dark channel. (a) Dark channel of DCP [12] approach. (b) Proposed scene-specific dark channel.

Where n is number of depth regions in that image. The proposed technique computes more robust scene-specific dark channel than the previous approaches. Figure 4 visualizes the effectiveness of our technique by comparing the scene-specific dark channel with dark channels of DCP and follow-up approaches. It is clearly seen that proposed scene-specific dark channel produces more robust results.

C. Atmospheric light Estimation

We have followed the similar procedure of DCP and other follow-ups for atmospheric light (**A**) estimation. This estimation process lies on the assumption of the intensity of brightest pixel is considered as the **A** in a foggy image. As the first step of estimating **A**, brightest pixels of the scene-specific dark channel are identified. Among them top 0.1% brightest pixels are selected, and their average intensity value is considered as the **A**. Since we have computed scene-specific dark channel and used it to estimate **A**, more robust results are obtained.

D. Scene-Specific Transmission Estimation

Transmission (*t*) indicates the amount of light that penetrates through the fog. Robust transmission estimation is important in all defogging frameworks since it is used to recover the fog-free image through equation 8. Based on equation 7, the transmission estimation process is mainly depending on the defogging parameter ω since it controls the degree of fog removal.

TABLE 2: Average intensities of regions and corresponding ω

In most of the approaches, ω is kept to a fixed value (0.95), and hence the fog removal process is conducted with equal probability in all the pixels of an image. However, we have notice that conducting fog removal with equal probability in all pixels will create unnatural effect in recovered image. The degree of fog removal should be large in dense fog regions and be small in thin fog regions. Based on that concept, we have used a novel technique, which is called as scene-specific transmission estimate.

Average Intensity (I_i)	**defogging parameter (ω)**
$I_i \geq 230$	0.95
$230 > I_i \geq 140$	0.9
$140 > I_i \geq 100$	0.8
$100 > I_i \geq 80$	0.7
$I_i < 80$	0.6

We have utilised the depth map regions, which were identified at the initial stage, to fix the density based local ω

values. The average intensity of each depth regions is computed and then corresponding local ω values are assigned. High values are assigned for high density fog regions and low values are assigned for low density regions. The details of this process are described in Table 2.

Based on the corresponding local defogging parameter, the scene-specific transmission calculation becomes:

$$t(x) = 1 - \omega_r \min_{y \in \Omega(x)} \left(\min_{c} \frac{I^c(y)}{A^c} \right), \quad (11)$$

Where ω_r is the region specific defogging parameter. The proposed technique removes more fog in high density regions while keeps few amounts of fog in thin density regions. Therefore, the recovered fog-free image becomes more natural than the previous approaches.

E. Recovering Scene Radiance

Similar to other approaches, scene radiance **J** is recovered by using the equation 8 in the proposed framework. The estimated scene-specific transmission is used to recover the fog-free image.

F. Post-Processing

We have used a post-processing technique to enhance the quality of the recovered image. Colour of the recovered fog-free image is improved by the histogram normalization technique. Figure 5 visualizes the proposed post-processing technique. It is clearly seen that the post-processing adjusts the colours and hence the recovered images becomes more realistic and natural.

(a) (b)

Fig.5. Histogram normalization based post-processing. (a) recovered fog-free image. (b) Enhanced post-processed image.

V. Experiments

A. Implementation details and Evalution Protocols

In the proposed work, all the ground truth and foggy images are resized to 500 × 500. The proposed approach is implemented in MATLAB. All comparisons are conducted on an Intel core i7-8550U CPU. The code and the results of this work are available at https://github.com/Kokul1984/Scene_Specific_Dark_Channel.

Mean-Squared Error (MSE), Peak Signal-To-Noise Ratio (PSNR) and Structural Similarity Index (SSIM) are the well-known metrices for evaluating the performance of defogging and dehazing frameworks. MSE calculates the average of the squares of the errors between ground truth (fog-free) image (**G**) and recovered image (**F**) by the following equation:

$$MSE = \frac{1}{M \times N} \sum_{i=1}^{M} \sum_{j=1}^{N} [\, F(i,j) - G(i,j) \,]^2, \quad (12)$$

Where M and N are the width and height of the image, respectively. PSNR measures the peak error as follow:

$$PSNR = 10 \log_{10} \left(\frac{MAX_G^2}{MSE} \right). \quad (13)$$

Where MAX_G is the maximum pixel value in the ground truth image. Since PSNR is depending on MSE, both metrices are producing similar results. The SSIM [33] index is used to measure the quality of an image based on a reference image. A high SSIM index represents high similarity between ground truth image and recovered fog-free image. In this evaluation, we have selected PSNR and SSIM to measure the distance error and the similarity between the ground truth image and the recovered image.

B. Dataset

In general, foggy images and corresponding ground truth (fog-free) images are important to evaluate the performance of defogging frameworks. However, it is difficult to obtain such kind of pairs of images and hence synthetic images are used to evaluate the recovering performance in many approaches. In this background, we have used the Foggy Road Image DAtaset (FRIDA) to evaluate the performance of the proposed approach and then compared it with state-of-the-art approaches.

There are 72 synthetic foggy images in the FRIDA benchmark, and they are created by adding different types of fogs on 18 ground truth images. Each image has the size of 640 × 480.

C. Testing results

The performance of the proposed defogging framework is compared with state-of-the-art single image defogging approaches on FRIDA benchmark. We compare the proposed approach with the works of Kim et al. [1], Pang et al. [13], He et al. [15], Kaiming et al. [14], Zhu et al. [2], He et al. [30] and Yu et al. [12]. In this comparison study, source codes of all approaches are obtained and evaluated on FRIDA benchmark with same parameter settings.

TABLE-3 Performance comparison on FRIDA benchmark

Approach	PSNR	SSIM
Ours	**14.5531**	**0.8225**
Kim et al. [1]	14.3187	0.8043
Zhu et al. [2]	13.9140	0.8051
Kaiming et al. [14]	12.9382	0.6192
He et al. [30]	12.7739	0.7182
He et al. [15]	12.4027	0.4273
Pang et al. [13]	12.1701	0.7921
Yu et al. [12]	11.0105	0.3758

Table 3 compares the performance of proposed single image defogging framework with other state-of-the-art approaches. It is clearly seen that our framework produces excellent defogging performance for both evaluation metrices. Figure 6 compares the qualitative results with well-performing approaches on few real-world images. Based on the figure, we can observe that proposed approach successfully removes the fog and produces more realistic and natural results.

(a) (b) (c) (d) (e) (f)

Fig.6. Comparison with other methods. (a) Input foggy image. (b) Kim [1]'s result. (c) Kaiming[14]'s result. (d) Zhu [2]'s results. (e) He [15]'s result. (f) Our result

VI. CONCLUSION

In this paper, we presented an image processing based simple but efficient framework for single image defogging. Based on the density of fog in local regions, we have obtained the rough depth map of a foggy image, and then used it to feed the scene-specific knowledge to defogging. In addition, we have proposed a scene-specific dark channel estimation technique and a transmission estimation technique, which are used to improve the recovering performance of the approach. The proposed defogging method shows state-of-the-art recovering performance on FRIDA benchmark dataset.

REFERENCES

[1] J.-H. Kim, W.-D. Jang, J.-Y. Sim, and C.-S. Kim, "Optimized contrast enhancement for real-time image and video dehazing," Journal of Visual Communication Image Representation vol. 24, pp. 410-425, 2013.

[2] Q. Zhu, J. Mai, and L. Shao, "A fast single image haze removal algorithm using color attenuation prior," IEEE transactions on image processing vol. 24, pp. 3522-3533, 2015.

[3] K. Sangkyoon, P. Soonyoung, and C. Kyoungho, "A system architecture for real time traffic monitoring in foggy video," in Proceedings of the 21st Korea-Japan Joint Workshop on Frontiers of Computer Vision (FCV), pp. 1-4, 2015.

[4] L. Tyron and M.Natasha, "Are you in the loop? Using gaze dispersion to understand driver visual attention during vehicle automation," Transportation Research Part C: Emerging Technologies, vol. 76, pp. 35-50, 2017.

[5] W. Chengjia, D. Shizhou, Z. Xiaofeng, P. Giorgos, Z. Heye, and Y. Guang, "Saliencygan: Deep learning semi-supervised salient object detection in the fog of iot," IEEE Transactions on Industrial Informatics, pp. 2667 - 2676, 2019.

[6] T. Kokul, C. Fookes, S. Sridharan, A. Ramanan, and U. A. J. Pinidiyaarachchi, "Target-specific siamese attention network for real-time object tracking," IEEE Transactions on Information Forensics and Security vol. 15, pp. 1276-1289, 2019.

[7] G. Woodell, D. J. Jobson, Z.-u. Rahman, and G. Hines, "Advanced image processing of aerial imagery," in Proceedings of the Visual Information Processing XV, p. 62460E, 2006.

[8] M. I. Anwar and A. Khosla, "Vision enhancement through single image fog removal," Engineering science technology, vol. 20, pp. 1075-1083, 2017.

[9] A. K. Tripathi and S. Mukhopadhyay, "Removal of fog from images: A review," IETE Technical Review, vol. 29, pp. 148-156, 2012.

[10] Y. Y. Schechner, S. G. Narasimhan, and S. K. Nayar, "Instant dehazing of images using polarization," in Proceedings of the IEEE Computer Society Conference on Computer Vision and Pattern Recognition. , pp. I-I, 2001.

[11] X. Li and Q. Huang, "Polarization filtering for automatic image dehazing based on contrast enhancement," in Proceedings of the IEEE 9th International Conference on Communication Software and Networks (ICCSN), pp. 1266-1271, 2017.

[12] S. Yu, H. Zhu, Z. Fu, and J. Wang, "Single image dehazing using multiple transmission layer fusion," Journal of Modern Optics, vol. 63, pp. 519-535, 2016.

[13] J. Pang, O. C. Au, and Z. J. P. A. A. Guo, "Improved single image dehazing using guided filter," APSIPA ASC, pp. 1-4, 2011.

[14] H. Kaiming, S. Jian, and T. Xiaoou, "Single image haze removal using dark channel prior," IEEE transactions on pattern analysis and machine intelligence, vol. 33, pp. 2341-2353, 2010.

[15] R. He, Z. Wang, H. Xiong, and D. D. Feng, "Single image dehazing with white balance correction and image decomposition," in Proceedings of the International Conference on Digital Image Computing Techniques and Applications (DICTA), pp. 1-7, 2012.

[16] Z. Ling, X. Li, W. Zou, and M. Liu, "Joint Haze-relevant Features Selection and Transmission Estimation via Deep Belief Network for Efficient Single Image Dehazing," in Proceedings of the 24th International Conference on Pattern Recognition (ICPR), pp. 133-139, 2018.

[17] Z. Li, B. Gui, T. Zhen, and Y. Zhu, "Grain depot image dehazing via quadtree decomposition and convolutional neural networks," Alexandria Engineering Journal, 2020.

[18] B. Cai, X. Xu, K. Jia, C. Qing, and D. Tao, "Dehazenet: An end-to-end system for single image haze removal," IEEE Transactions on Image Processing, vol. 25, pp. 5187-5198, 2016.

[19] V. Thulasika and A. Ramanan, "Single Image Fog Removal based on Fusion Strategy," Digital Image Processing and Pattern Recognition (DPPR), pp. 115-123, 2015 2015.

[20] N. Bharath Raj and N. Venkateswaran, "Single Image Haze Removal using a Generative Adversarial Network," arXiv preprint arXiv:.09479, 2018.

[21] A. Kumari, P. J. Thomas, and S. Sahoo, "Single image fog removal using gamma transformation and median filtering," in Proceedings of the Annual IEEE India conference (INDICON), pp. 1-5, 2014.

[22] Z. Xu, X. Liu, and N. Ji, "Fog removal from color images using contrast limited adaptive histogram equalization," in Proceedings of the International Congress on Image and Signal Processing, pp. 1-5, 2009.

[23] J. Yu and Q. Liao, "Fast single image fog removal using edge-preserving smoothing," in Proceedings of the IEEE International Conference on ICASSP, pp. 1245-1248, 2011.

[24] J.-P. Tarel, N. Hautiere, A. Cord, D. Gruyer, and H. Halmaoui, "Improved visibility of road scene images under heterogeneous fog," in Proceedings of the IEEE Intelligent Vehicles Symposium, pp. 478-485, 2010.

[25] N. Hautière, J.-P. Tarel, H. Halmaoui, R. Brémond, and D. Aubert, "Enhanced fog detection and free-space segmentation for car navigation," Machine vision applications, vol. 25, pp. 667-679, 2014.

[26] M. K. Saggu and S. Singh, "A review on various haze removal techniques for image processing," International journal of current engineering technology, vol. 5, pp. 1500-1505, 2015.

[27] G. Yadav, S. Maheshwari, and A. Agarwal, "Fog removal techniques from images: A comparative review and future directions," in Proceedings of the International Conference on Signal Propagation and Computer Technology, pp. 44-52, 2014.

[28] R. Sharma and V. Chopra, "A review on different image dehazing methods," International Journal of Computer Engineering Applications, vol. 6, p. 11, 2014.

[29] C. Chen, J. Li, S. Deng, F. Li, and Q. Ling, "An adaptive image dehazing algorithm based on dark channel prior," in Proceedings of the 29th Chinese Control And Decision Conference (CCDC), pp. 7472-7477, 2017.

[30] K. He, J. Sun, and X. Tang, "Guided image filtering," in Proceedings of the European conference on computer vision, pp. 1-14, 2010.

[31] S. G. Narasimhan and S. K. Nayar, "Vision and the atmosphere," International journal of computer vision vol. 48, pp. 233-254, 2002.

[32] R. Achanta, A. Shaji, K. Smith, A. Lucchi, P. Fua, and S. Süsstrunk, "SLIC superpixels compared to state-of-the-art superpixel methods," IEEE transactions on pattern analysis machine intelligence, vol. 34, pp. 2274-2282, 2012.

[33] Z. Wang, A. C. Bovik, H. R. Sheikh, and E. P. Simoncelli, "Image quality assessment: from error visibility to structural similarity," IEEE transactions on image processing, vol. 13, pp. 600-612, 2004.